International Journal of Multimedia and Ubiquitous Engineering
Vol.11, No.3 (2016), pp.23-36
http://dx.doi.org/10.14257/ijmue.2016.11.3.03

Research on AC Servo Motor Load Disturbance Method

Xiao Qianjun[1] and Zhang Xiaoqin[1]

1. Chongqing Industry Polytechnic College, Chongqing 401120, China
E-mail

Abstract

For the decline of the control accuracy of servo system due to the disturbances of load, to design the dimensionality reduction load torque observer, the observed value of load torque after conversion for compensation control. Established the three- loop mathematical model of servo control system, to elicit three- loop control parameter setting formula by the application of optimal second order and third order model theory. Established the simulation model of space vector control AC servo system, by simulation experiment it is verified that three-ring parameters can provide good dynamic performance for system after setting. After the establishment of experimental platform, through the motor load sudden change experiment, it proved the feasibility of the torque compensation control for improving the servo system control precision under load disturbances.

Keywords*: Servo system; Observer; Load disturbance; Parameters setting*

1. Introduction

With the rapid and continuous development of the technical fields such as electronic power, microcomputer, microelectronics and sensor, *etc.*, the performance of the AC servo motor has been improved substantially [1], for its speed control of high performance, high precision and wide range, and its growing demand in industries such as aerospace, rail transportation, oil drilling, wind power generation, marine propulsion, electric vehicle, [2-3] *etc.* However, In the process of practical operation of servo system, load disturbance has adverse impact on the control accuracy of servo system. In order to make the system can be better suppressed this bad influence, it must be setting the three-loop control parameter on the system for its good disturbance rejection and dynamic response; Second, the design of the load torque observer, its observed value can be used as the dynamic compensation of the servo system. Based on the high observation precision of Kalman filtering observer, but the influence of high order mathematical model, which causes more parameters need to be adjusted, so the calculation is great. Although the sliding mode observer has good robustness, but its essence of discontinuous switch control, will cause the jitter of the system.

This paper adopts the theory of the optimal second order and third order model to elicit the setting formula of system three-loop control parameters; the method of reconstruct the state space, for the design of Luenberger dimensionality reduction observer, on the premise of maintain the observation accuracy, it reduced the amount of calculation, and the rapid response speed of the observer, can better observe the load torque.

2. Servo System Control Structure

Servo system control structure as shown in Figure 1, it adopts the three closed loop control system, from the inner to outer, respectively as the current loop, speed loop and position loop. The load torque observed by load observer is introduced into the input end of current regulator, as a compensation control input of load disturbance.

ISSN: 1975-0080 IJMUE

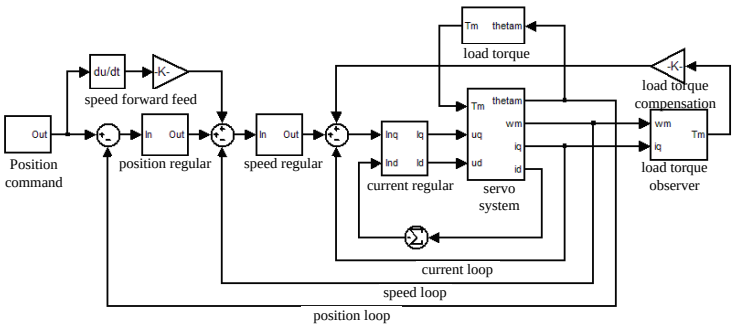

Figure 1. Servo System Three-Loop Control Structure

Position command, position regular, speed forward feed, speed regular, position loop, speed loop, current loop, servo system, load torque, load torque compensation, load torque observer

The output voltage of current regulator through space vector coordinate is transformed into a three-phase voltage of the motor to control the motor. After coordinate transformation and the magnetic field orientation method for the deflation of mathematical model of AC motor, the voltage equation of AC servo motor as follows:

$$u_q = R_s i_q + L_q \frac{di_q}{dt} + p_n \omega_m \psi_f \tag{1}$$

Electromagnetic torque equation as:

$$T_e = p_n[\psi_f i_q + (L_d - L_q) i_d i_q] \tag{2}$$

For $i_d = 0$, the above equation changed to:

$$T_e = p_n \psi_f i_q = K_T i_q \tag{3}$$

System motion equation as:

$$J \frac{d\omega_m}{dt} = T_e - T_L \tag{4}$$

In the above equation, T_e represents servo motor electromagnetic torque, R_s represents motor stator resistance, ω_m represents motor speed, u_d, u_q, i_d, i_q, L_d, L_q represent motor stator d and q axis equivalent voltage, current and inductor, respectively, ψ_f represents permanent magnet rotor flux linkage, p_n represents number of pole-pairs, T_L represents load torque, K_T represents torque constant.

3. Design Principle of Dimensionality Reduction Load Torque Observer

According to the design method of linear time-invariant systems to design the motor load torque observer, due to the sampling frequency of current loop is greater than the change frequency of load torque, the load torque can be considered as the same within a sampling period, then $\dot{T}_l \approx 0$ [6] Simultaneous motor voltage equation, electromagnetic torque equation and motion equation of the motor rotor, the obtained observer equation as follows:

$$\begin{bmatrix} \dot{i}_q \\ \dot{\omega}_m \\ \dot{T}_l \end{bmatrix} = \begin{bmatrix} -\frac{R_s}{L} & -\frac{K_E}{L} & 0 \\ \frac{K_T}{J} & 0 & -\frac{1}{J} \\ 0 & 0 & 0 \end{bmatrix} \begin{bmatrix} i_q \\ \omega_m \\ T_l \end{bmatrix} + \begin{bmatrix} \frac{1}{L} \\ 0 \\ 0 \end{bmatrix} u_q \tag{5}$$

That is:

$$\dot{x} = Ax + Bu$$

Let output as:

$$y = \begin{bmatrix} i_q \\ \omega_m \end{bmatrix} = \begin{bmatrix} 1 & 0 & 0 \\ 0 & 1 & 0 \end{bmatrix} \begin{bmatrix} i_q \\ \omega_m \\ T_l \end{bmatrix} = Cx \tag{6}$$

Where A,B,C are constant matrix.

$$x = \begin{bmatrix} i_q & \omega_m & T_l \end{bmatrix}^T, y = \begin{bmatrix} i_q & \omega_m \end{bmatrix}, u = u_q \circ$$

For $rank(N) = rank(\begin{bmatrix} C & CA & CA^2 \end{bmatrix}) = 3$, so the state of the observer is a universal observation, the observer exists, state observer can be designed. For the system state space expression as:

$$\begin{bmatrix} \dot{x}_1 \\ \dot{x}_2 \end{bmatrix} = \begin{bmatrix} A_{11} & A_{12} \\ A_{21} & A_{22} \end{bmatrix} \begin{bmatrix} x_1 \\ x_2 \end{bmatrix} + \begin{bmatrix} B_1 \\ B_2 \end{bmatrix} u, \quad y = \begin{bmatrix} C_1 & C_2 \end{bmatrix} x$$

Where:

$$x_1 = y = \begin{bmatrix} i_q \\ \omega_m \end{bmatrix}, \quad x_2 = T_l, \quad A_{11} = \begin{bmatrix} -\frac{R_s}{L} & -\frac{K_E}{L} \\ \frac{K_T}{J} & 0 \end{bmatrix}, \quad A_{12} = \begin{bmatrix} 0 \\ -\frac{1}{J} \end{bmatrix}, \quad A_{21} = \begin{bmatrix} 0 & 0 \end{bmatrix}, \quad A_{22} = 0,$$

$$B_1 = \begin{bmatrix} \frac{1}{L} \\ 0 \end{bmatrix}, \quad B_2 = 0, \quad C_1 = \begin{bmatrix} 1 & 0 \\ 0 & 1 \end{bmatrix}, \quad C_2 = \begin{bmatrix} 0 \\ 0 \end{bmatrix} \circ$$

Due to variable x_1 is the state can be directly observed value, while variable x_2 is the state cannot be directly observed value, that is load torque T_l as the observed value to establish a 1-D observer. The expression equation of the system state space of dimensionality reduction observer as:

$$\begin{cases} \dot{x}_2 = A_{21}x_1 + A_{22}x_2 + B_2u \\ \dot{y} = A_{11}x_1 + A_{12}x_2 + B_1u \end{cases} \tag{7}$$

According to the design idea of dimensionality reduction observer, it can be obtained dimensionality reduction observer expression as:

$$\begin{aligned} \dot{\hat{x}}_2 &= A_{21}x_2 + A_{22}\hat{x}_2 + B_2u \\ &-L(A_{11}x_1 + A_{12}\hat{x}_2 + B_1u - \dot{x}_1) \end{aligned} \tag{8}$$

Where the observer gain matrix is $L = \begin{bmatrix} l_1 & l_2 \end{bmatrix}$, it should reasonably design the value of observer gain matrix to make the observer system stable and respond fast. State estimation error of the system as $e = x_2 - \hat{x}_2$, then obtained error rate as:

$$\dot{e} = \dot{x}_2 - \dot{\hat{x}}_2 = (A_{22} - LA_{12})(x_2 - \hat{x}_2) \tag{9}$$

If let $\lim_{t\to\infty} e = \lim_{t\to\infty} | x_2 - \hat{x}_2 | = 0$, the system is stable. Therefore, it needs to let matrix $A_{22} - LA_{12}$ has appropriate characteristic value, the error has a certain attenuation rate[9]. for $\det(sI - (A_{22} - LA_{12})) = s - \frac{1}{J} l_2$, thus this problem is translated into the pole assignment problem of the system. Only $l_2 < 0$, the observer is stable then. And the greater of the absolute value of l_2, the expectation pole of the system is further away from the imaginary axis, and the response speed of the observer is faster, the vibration frequency increased, and vice versa [8].

As variable substitution $l_2 = -pJ$, and integral the equation (9), obtained the final expression of dimensionality reduction observer as:

$$\hat{T}_l = p(J\omega_m + \frac{\hat{T}_l}{s} - \frac{K_T i_q}{s}) \tag{10}$$

To establish dimensionality reduction load torque observer model based on equation (10), as shown in Figure 2.

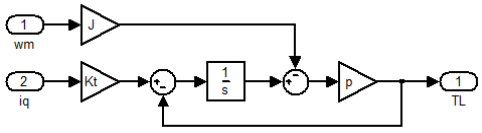

Figure 2. Dimensionality Reduction Load Torque Observer Model

4. Control Parameters Setting of Servo System

Servo system adopts three-loop cascade control structure, different control link has different characteristic and property, therefore, it needs to establish a mathematical model of each control link, and then setting the control parameters setting of servo system according to the mathematical model.

4.1. Control Parameters Setting of Current Loop

According to the control principle of space vector, current loop is divided into field current loop and torque current loop, the aim of the torque current loop is for obtaining the fast and high precision torque control, field current loop is designed to make the motor obtained the approximate decoupling in the running process. Although two current loops are independent, but the control mode of field current loop and torque current loop is the same, so their control parameter settings are the same. Torque current loop includes the feed forward filter and feedback filter, PWM inverter, current loop regular, the armature winding, *etc*., based on each link of the current loop and the analysis of the control process, the current loop control model is set up as shown in Figure 3.

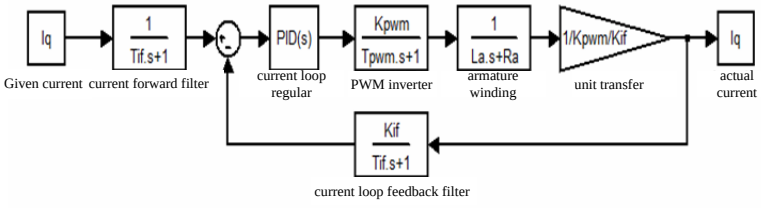

Figure 3. Current Loop Structure Control Chart

Given current, current forward filter, current loop regular PWM inverter, current loop feedback filter, armature winding, unit transfer, actual current.

It can be known from Figure 3, open-loop transfer function of current loop as:

$$G_{iK}(s) = \frac{K_R K_i (T_i s + 1)}{(T_{pwm} s + 1)(T_L s + 1)(T_{if} s + 1) T_i s} \tag{11}$$

Where, T_{if} represents time constant of current filter, K_{pwm} represents amplification coefficient of inverter, T_{pwm} represents time constant of PWM, L_a represents stator phase inductance, R_a represents stator phase resistance, current loop controller adopts PI control method, its transfer function as:

$$K_i (1 + \frac{1}{T_i s})$$

Where, K_i is proportional gain of current loop, T_i is the integral time constant of current loop.

Due to both filter time constant T_{if} and switching period T_{pwm} are small time constant, inductance time constant T_L is far larger than T_{if} and T_{pwm}. Use a first-order inertial of time constant T_{ic} to replace these two inertial element, combined small intertal element, let:

$$T_{ic} = T_{if} + T_{pwm} \tag{12}$$

Then equation (11) can be changed to:

$$G_{iO}(s) = \frac{K_R K_i (T_i s + 1)}{(T_L s + 1)(T_{ic} s + 1) T_i s} \tag{13}$$

For offset the system delays caused by the big inertia element, so as to improve the response speed, it can take:

$$T_i s + 1 = T_m s + 1 \tag{14}$$

Then equation (13) is changed to:

$$G_{iO}(s) = \frac{K_R K_i}{(T_{ic} s + 1) T_i s} \tag{15}$$

The primary goal of current loop control parameters setting is to make the current loop to obtain good dynamic and steady-state performance, so the current loop should be open loop correction into typical type I system, taking:

$$\frac{K_R K_i T_{ic}}{T_i} = 0.5 \tag{16}$$

Where, the time constant of PWM inverter is 100us, the time constant of current filter is 200us, the specific parameters of the motor refer to Table 1.

Table 1. Permanent Magnet Synchronous Motor Parameters

parameter name	symbol (unit)	
rated torque	M_n[Nm]	10.0
maximum torque	M_{max}[Nm]	30.0
torque constant	K_T[Nm/A]	2.49
back EMF coefficient	K_E[mVmin]	151
stator phase resistance	R_a[Ω]	4.13
stator phase inductance	L_a[mH]	24.0
rotor intertia	J[kgcm^2]	27.4

pole-paris	p	10

To substitute data from Table 1 into equation (14) and (16), obtained control parameters of current regular $T_i = 5.8ms$, $K_i = 40V / A$.

The unit step response and frequency response characteristic of current loop as shown in Figure 4 and 5, respectively, the maximum overshoot of unit step response of current loop is 4.56%, setting time is 61ms, and the current loop bandwidth frequency is 2.65MHz.

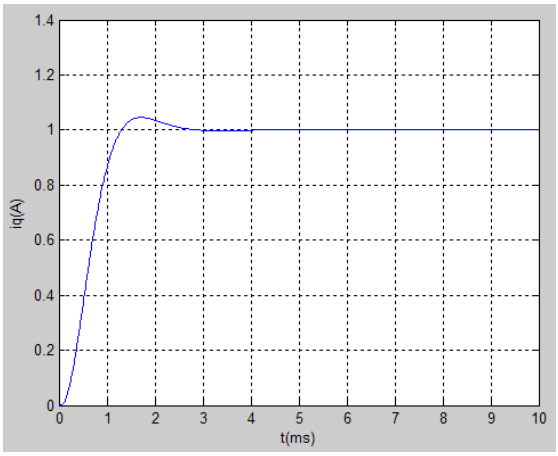

Figure 4. Unit Step Response of Current Loop

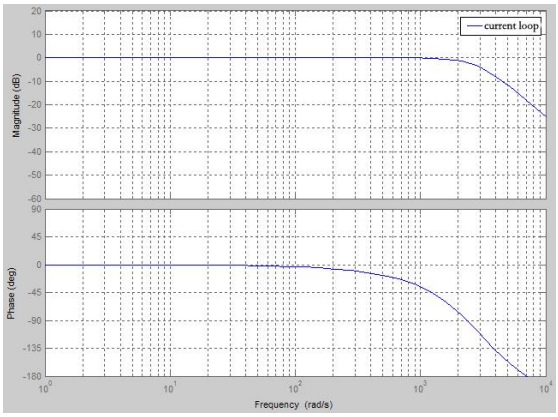

Figure 5. Frequency Response Characteristic of Current Loop

Due to the cut-off frequency of the speed loop of servo system is usually smaller than cut-off frequency of the current loop, so in the design of speed regulator, current closed-loop can be equivalent to a first-order inertia element, taking:

$$G_{iC}(s) = \frac{1}{2T_i s + 1} \tag{17}$$

4.2. Parameter Setting of Speed Loop Control

The function of speed loop is to eliminate the effect of load torque disturbance and other factors on motor speed, guarantee the actual speed is consistent with the order speed value. Speed loop mainly consists of current loop, speed regulator, servo motor, load object, load torque observer, feedforward filter and feedback filter, *etc.*, based on the

analysis of each component part and the control process of speed loop, the established speed loop control model is shown in Figure 6.

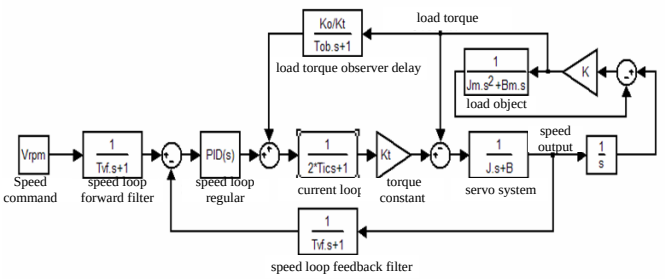

Figure 6. Speed Loop Structure Control Chart

Speed command, speed loop forward filter, speed loop regular, current loop, speed loop feedback filter, load torque observer delay, load torque, torque constant, load object, speed output, servo system

The speed loop regular adopts PI control method, its transfer function as:

$$K_v(1+\frac{1}{T_v s})$$

Where: K_v is the proportional gain of current loop, T_v is the current loop integral time constant.

Assuming that the load torque observation can be fully compensated the load torque disturbance, the viscous coefficient of servo motor is neglected, merged small inertia element, let $T_{vc} = T_{vf} + 2 * T_{ic}$, then obtained open-loop transfer function of speed loop as:

$$G_{vO}(s) = \frac{K_v K_T (T_v s + 1)}{T_v (T_{vc} s + 1) J s^2} \tag{18}$$

In the equation, T_{vf} represents time constant of current filter, K represents stiffness coefficient of mechanical transmission element, J_m represents load rotational intertia, B_m represents load coefficient of viscosity, T_{ob} represents observed response time of load torque, Usually set the response speed of the observer 3 ~ 10 times faster than state feedback system (*i.e.*, the current loop), take：$T_{ob} = 1/3T_{ic}$, K_o is the proportional gain of torque compensation,

Speed loop is a very important part of the servo system, speed loop requires to realize no static difference on the steady state performance, and has high precision and fast response on the dynamic performance, at the same time has good load disturbance resistance, so the speed loop should be designed in accordance with the standard type II system [4].

To define variable h as the intermediate frequency bandwidth of the system, $h = 4$ the setting time of the system is the shortest, and disturbance-rejection ability is the strongest, then:

$$T_v = hT_{vc} = 5T_{vc} \tag{19}$$

$$K_v = \frac{(h+1)J}{2hK_T T_{vC}} \tag{20}$$

It can make setting on speed loop regular according to equation (19), (20), obtained control parameter of speed regular:

$$T_v = 18\text{ms}\ K_v = 0.46 Nm \cdot s / rad\ 。$$

Unit step response and the frequency response characteristic of the speed loop shown in Figure 7-8, respectively, the maximum overshoot of speed loop unit step response is 34.36%, the biggest setting time is 46 ms, and speed loop bandwidth frequency is 247 Hz.

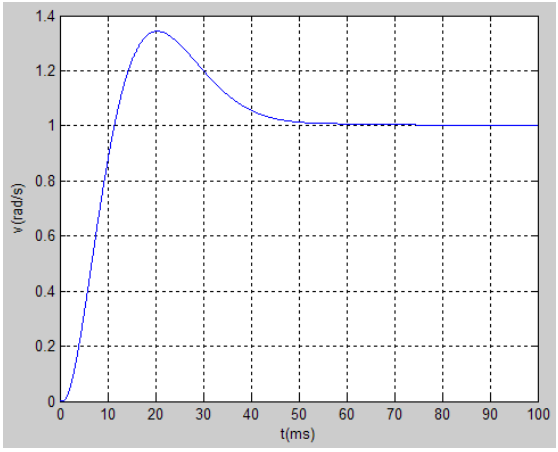

Figure 7. Speed-Loop Unit Step Response

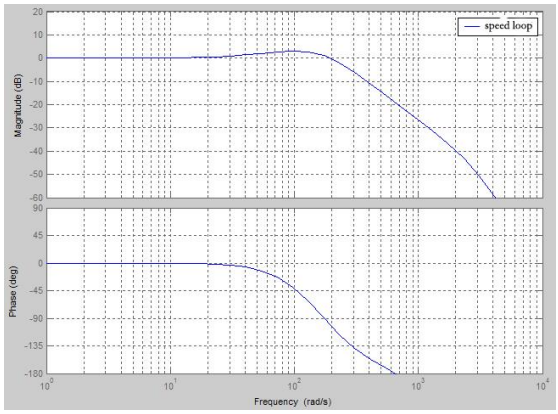

Figure 8. Speed Loop Frequency Response Characteristic

After parameter setting, open-loop transfer function of speed loop as:

$$G_{vO}(s) = \frac{4T_{vc}s + 1}{4T_{vc}^2 s^2 (T_{vc}s + 1)} \tag{21}$$

Closed-loop transfer function of speed loop as:

$$G_{vB}(s) = \frac{4T_{vc}s + 1}{8T_{vc}^2 s^2 (T_{vc}s + 1) + (4T_{vc}s + 1)}$$

$$G_{vB}(s) \approx \frac{1}{2T_{vc}s + 1} \tag{22}$$

It can be seen from equation (22), after parameter setting, closed-loop transfer function of speed loop can be approximate to the first-order inertia element.

4.3. Position Loop Control Parameters Setting

Position loop is located at the outer loop, the complete position follow –up and positioning function, so it requires rapid positioning and good follow-up ability. As the continuous tracking control, position loop cannot have overshoot, therefore, generally adopts the compound control method of proportional control + feedforward [5].

According to above analysis, the obtained position loop control structure is shown as Figure 9.

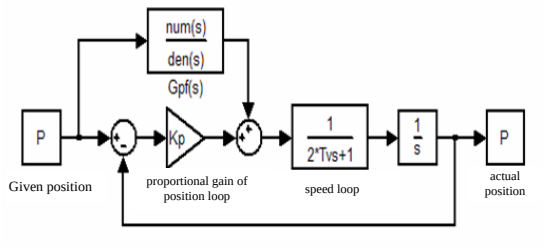

Figure 9. Position Loop Structure Control Chart

Given position, proportional gain of position loop, speed loop, actual position
The open-loop transfer function of position loop as:

$$G_{pO}(s) = \frac{G_{pf}(s) + K_p}{(2T_v s + 1)s} \tag{23}$$

Where, K_p indicates proportional gain of the position loop, $G_{pf}(s)$ is the transfer function of the feedforward part, we obtained transfer function of position closed-loop as:

$$G_{pB}(s) = (1 + \frac{G_{pf}(s)}{K_p}) \frac{K_p}{(2T_v s + 1)s} \tag{24}$$

When conducting control parameter setting of position loop, the influence of feedforward gain on the performance of the position loop shall not be considered, but correct the position loop into typical type I system, and no overshoot is allowed in the process of position control [8], it should be satisfied:

$$K_p \cdot 2T_v = 0.2 \tag{25}$$

Obtained proportional gain of position loop: $K_p = 28.8s^{-1}$

The unit step response and frequency response characteristics of position loop respectively as shown in Figure 10, 11, there is no overshoot exists the position loop step response, and when the adjustment time is 150 ms, its bandwidth frequency is 40.6 Hz.

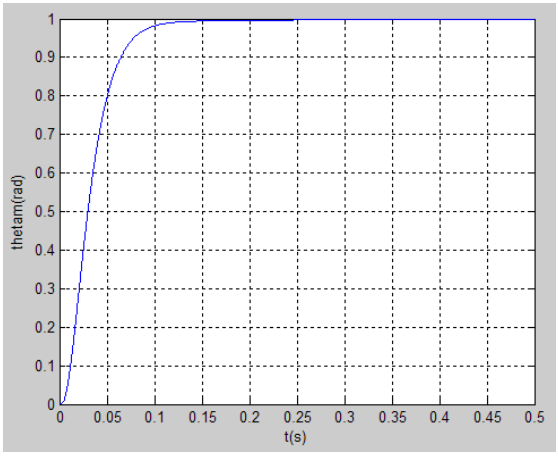

Figure 10. Position Loop Unit Step Response

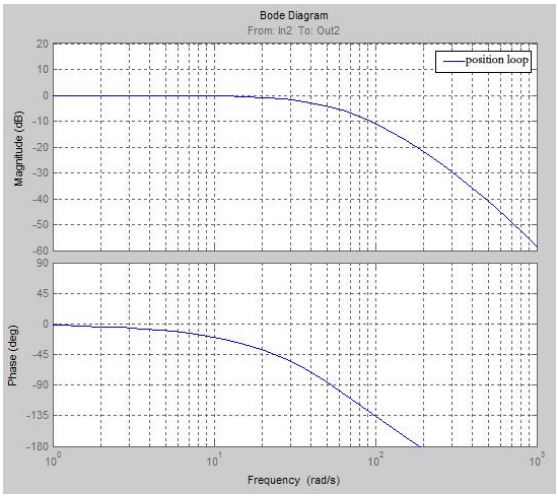

Figure 11. Position Loop Frequency Response Characteristics Position Loop

5. Simulated Analysis

5.1. The Establishment of Simulation Model

As shown in Figure1, to establish the simulation model of servo motor. Where, observed value of load torque $\hat{T}_m$ can be equivalent to current value of q axle, as the input of current regulator for compensation control, the influence of the change of compensation load torque on the accuracy of servo motor position.

5.2. Velocity Curve at the Motor Starting

When motor starts, the velocity cureve will directly affect the position precision of system transition process, the transition process should try to ensure no sudden change of load torque, which requires no sudden change of motor accelerated velocity in the transition process, so S-shaped velocity curve can meet the above requirements. The servo system is mainly take multiaxial drum institution of cigarette-rolling machine as the research object, the speed of motor should be up to 400 r/min to meet the actual production requirement. If the motor speed reaches more than 400 r/min after 1.4 s, the expression of S-type curve as:

$$\omega_m = \begin{cases} 5000t^2 & t \le 0.2 \\ 2000t - 200 & 0.2 < t \le 1.2 \\ -5000t^2 + 14000t - 7400 & 1.2 < t \le 1.4 \\ 2400 & t > 1.4 \end{cases}$$

Where, t is the time variable, the unit of motor speed ω_m is $^\circ / s$, the velocity curve as shown in Figure 12.

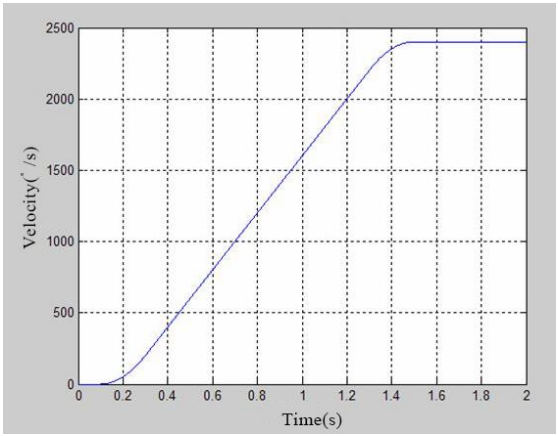

Figure 12. Velocity Curve at the Motor Starts Velocity, Time

5.3. Analysis of Simulation Result

To verify the effect of the designed dimensionality reduction load observer and compensation control, respectively simulate the system before and after adding compensation control. After motor starts, the observation curve of load torque as shown in Figure 13, after motor speed stability, then add triangle wave load disturbance, the observation curve as shown in Figure 14.

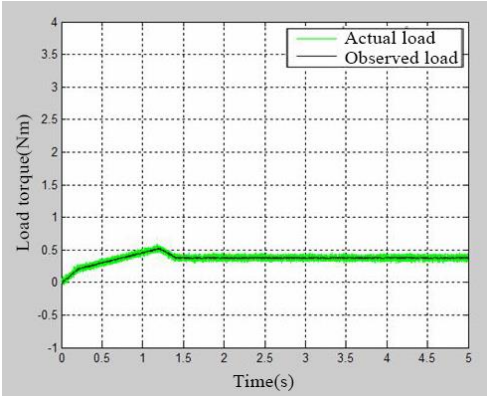

Figure 13. Observation Curve of Motor Starting Load Torque, Actual Load, Observed Load

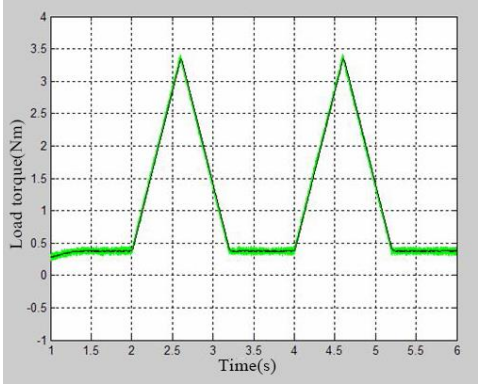

Figure 14. Observation Curve after Adding Torque Disturbance Load Torque, Time

It can be seen from the Figure, the observed value of load torque can better track the actual load torque value, no overshoot, short response time, and good static and dynamic performances.

When the motor starts, the change of load torque value has direct influence on the accuracy of motor position, Figure 15 and 16 are the position error curve of no adding torque compensation and adding torque compensation, respectively, add load disturbance after motor sped stabilized, Figure 17 and 18 are the position error curve of no adding torque compensation and adding torque compensation, respectively.

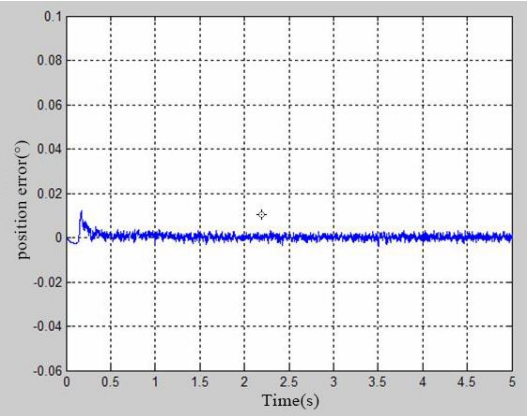

Figure 15. Position Error before Compensation

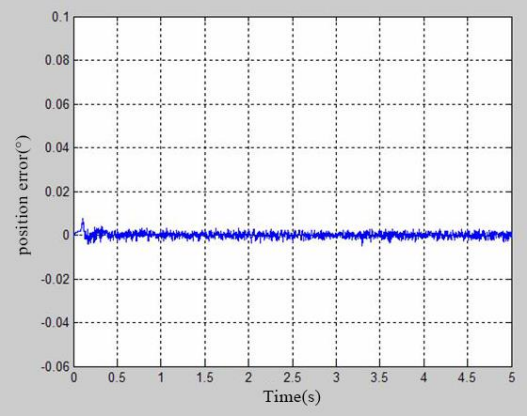

Figure 16. Position Error after Compensation

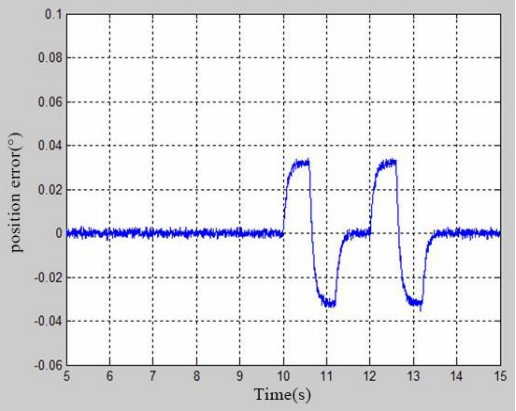

Figure 17. Position Error before Compensation

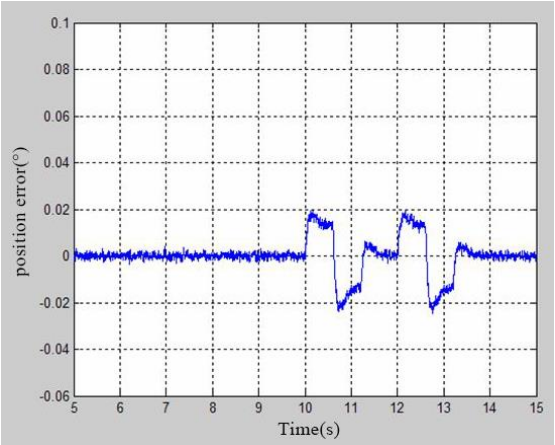

Figure 18. Position Error after Compensation

It can be seen that, after adding compensation, the maximum error of motor position was somewhat reduced, and the setting time required back to steady state was somewhat decreased, so the ability of motor resistance to load disturbance was obvious improved.

Table 2. Analysis of Simulation Result of Motor Resistance to Load Disturbance

add torque compensation or not	Position error at the motor starts (°)	Position error after adding load disturbance (°)
No	0.0172	0.0336
Yes	0.0085	0.0198

6. Conclusion

Based on the establishment of mathematical model of AC permanent magnet synchronous motor servo system, setting the control parameters of the servo system, and design dimensionality reduction load torque observer, restrain to compensate and control load torque disturbance for the motor. Both simulation and experimental results show that after parameters setting, the system has good robustness. After adding observer compensation control, the maximum error produced by servo system under the condition of the sudden change of load torque was decreased, meanwhile the setting time required to back to steady state was also reduced, thus the ability of the servo system to resistance to load disturbance was improved accordingly.

Acknowledgement

This work was supported by the Science and technology research project of Chongqing Municipal Education Commission (KJ102102).

Reference

[1] Z. Dongfang, “Fusion FS: Toward supporting data-intensive scientific applications on extreme-scale high-performance computing systems”, Big Data (Big Data), 2014 IEEE International Conference on. IEEE, **(2014)**.
[2] S. Dang, J. Ju, D. Matthews, X. Feng and C. Zuo, “Efficient solar power heating system based on lenticular condensation. Information Science, Electronics and Electrical Engineering (ISEEE)”, 2014 International Conference on, **(2014)**.
[3] Y. Wang, Y. Su and G. Agrawal, “A Novel Approach for Approximate Aggregations Over Arrays”, In Proceedings of the 27th international conference on scientific and statistical database management, ACM, **(2015)**.

[4] J. Hu and Z. Gao, "Modules identification in gene positive networks of hepatocellular carcinoma using Pearson agglomerative method and Pearson cohesion coupling modularity", Journal of Applied Mathematics, **(2012)**.
[5] X. Li, Z. Lv, J. Hu, L. Yin, B. Zhang and S. Feng, "Virtual Reality GIS Based Traffic Analysis and Visualization System", Advances in Engineering Software, **(2015)**.
[6] Z. Lv, C. Esteve, J. Chirivella and P. Gagliardo, "Clinical Feedback and Technology Selection of Game Based Dysphonic Rehabilitation Tool", 2015 9th International Conference on Pervasive Computing Technologies for Healthcare (PervasiveHealth2015), IEEE, **(2015)**.
[7] W. Ke, "Next generation job management systems for extreme-scale ensemble computing", Proceedings of the 23rd international symposium on High-performance parallel and distributed computing. ACM, **(2014)**.
[8] L. Tonglin, "Distributed Key-Value Store on HPC and Cloud Systems", 2nd Greater Chicago Area System Research Workshop (GCASR), **(2013)**.
[9] X. Zhang, Y. Han, D. Hao and Z. Lv, "ARPPS: Augmented Reality Pipeline Prospect System", 22th International Conference on Neural Information Processing (ICONIP), Istanbul, Turkey. In press, **(2015)**.
[10] W. Ou, Z. Lv and Z. Xie, "Spatially Regularized Latent topic Model for Simultaneous object discovery and segmentation", The 2015 IEEE International Conference on Systems, Man, and Cybernetics (SMC), **(2015)**.
[11] W. Wang, Z. Lu, X. Li, W. Xu, B. Zhang and X. Zhang, "Virtual Reality Based GIS Analysis Platform", 22th International Conference on Neural Information Processing (ICONIP), Istanbul, Turkey, **(2015)**.
[12] T. Su, W. Wang, Z. Lv, W. Wu and X. Li, "Rapid Delaunay Triangulation for Random Distributed Point Cloud Data Using Adaptive Hilbert Curve", Computers & Graphics, **(2015)**.
[13] J. Hu, Z. Gao and W. Pan, "Multi-angle Social Network Recommendation Algorithms and Similarity Network Evaluation", Journal of Applied Mathematics, **(2013)**.
[14] Z. Lv, T. Yin, Y. Han, Y. Chen and G. Chen, "WebVR——web virtual reality engine based on P2P network", Journal of Networks, vol. 6, no. 7, **(2011)**, pp. 990-998.
[15] N. Lu, C. Lu, Z. Yang and Y. Geng, "Modeling Framework for Mining Lifecycle Management", Journal of Networks, vol. 9, no. 3, **(2014)**, pp. 719-725.
[16] J. Hu and Z. Gao, "Distinction immune genes of hepatitis-induced heptatocellular carcinoma", Bioinformatics, vol. 28, no. 24, **(2012)**, pp. 3191-3194.
[17] W. Ke, "Overcoming Hadoop Scaling Limitations through Distributed Task Execution".
[18] Z. Su, X. Zhang and X. Ou, "After we knew it: empirical study and modeling of cost-effectiveness of exploiting prevalent known vulnerabilities across IAAS cloud", Proceedings of the 9th ACM symposium on Information, computer and communications security. ACM, **(2014)**.
[19] G. Bao, L. Mi, Y. Geng and K. Pahlavan, "A computer vision based speed estimation technique for localizing the wireless capsule endoscope inside small intestine", 36th Annual International Conference of the IEEE Engineering in Medicine and Biology Society (EMBC), **(2014)**.
[20] W. Gu, Z. Lv and M. Hao, "Change detection method for remote sensing images based on an improved Markov random field", Multimedia Tools and Applications, **(2016)**.
[21] Z. Lu, C. Esteve, J. Chirivella and P. Gagliardo, "A Game Based Assistive Tool for Rehabilitation of Dysphonic Patients", 3rd International Workshop on Virtual and Augmented Assistive Technology (VAAT) at IEEE Virtual Reality 2015 (VR2015), Arles, France, IEEE, **(2015)**.
[22] Z. Chen, W. Huang and Z. Lv, "Uncorrelated Discriminant Sparse Preserving Projection Based Face Recognition Method", Multimedia Tools and Applications, **(2016)**.

Author

Xiao Qian Jun, He was born in Chongqing, China, in 1974. He received the M.S degree in 2006 from Chongqing University of Posts and Telecommunications, China, in 2006. He joined Chongqing Industry Polytechnic College, in 2013, associate professor in Chongqing Industry Polytechnic College. His main research include Control theory and embedded system design.

